JOURNAL OF GEOPHYSICAL RESEARCH, VOL. 102, NO. D6, PAGES 6823-6830, MARCH 27, 1997

Wonderland climate model

J. Hansen, R. Ruedy, A. Lacis, G. Russell, M. Sato, J. Lerner, and D. Rind

NASA Goddard Institute for Space Studies, New York

P. Stone

Center for Meteorological and Physical Oceanography,
Massachusetts Institute of Technology, Cambridge

Abstract. We obtain a highly efficient global climate model by defining a sector version (120° of longitude) of the coarse resolution Goddard Institute for Space Studies model II. The geography of Wonderland is chosen such that the amount of land as a function of latitude is the same as on Earth. We show that the zonal mean climate of the Wonderland model is very similar to that of the parent model II.

1. Introduction

The climate system of the Earth provides a beautiful example of limited chaos, a combination of deterministic behavior and unpredictable fluctuations or noise. All parts of the system are connected by interactions and feedbacks, which give rise to exceedingly complex changing spatial patterns which never precisely repeat. The smallest alteration of initial or boundary conditions quickly changes the developing patterns, and thus next year's weather at any particular place is inherently unpredictable. The complex behavior arises from the coupling of the fundamental conservation equations which govern the structure and dynamics of the system [*Lorenz, 1963*]. Yet these same basic laws limit the range of behavior and help determine a mean deterministic response to a forcing of the system.

A climate model provides a tool which allows us to think about, analyze, and experiment with a facsimile of the climate system in ways which we could not or would not want to experiment with the real world. As such, climate modeling is complementary to basic theory, laboratory experiments, and global observations. Each of these tools has severe limitations, but together, especially in iterative combinations, they allow our understanding to advance.

Climate models, even though very imperfect, are capable of containing much of the complexity of the real world and the fundamental principles from which that complexity arises. Thus models can help structure the discussions and define needed observations, experiments, and theoretical work. For this purpose it is desirable that the stable of modeling tools include global climate models which are fast enough to allow the user to play games, to make mistakes and rerun the experiments, to run experiments covering hundreds or thousands of simulated years, and to make the many model runs needed to explore results over the full range of key parameters. Thus there is great incentive for development of a highly efficient global climate model, i.e., a model which numerically solves the fundamental equations for atmospheric structure and motion.

The model we define here is based on Goddard Institute for Space Studies (GISS) model II [*Hansen et al.*, 1983, hereafter paper 1], which is already quite efficient when used at coarse resolution. We increase the efficiency further here by employing the sector geometry introduced by *Manabe* [1969], i.e., the model grid is defined over only 120° of longitude, and the fundamental equations on a sphere are solved by assuming two other identical sectors.

We define an idealized geography for Wonderland, such that the amounts of land cover and ocean as a function of latitude are the same as for Earth. This characteristic is important for studies in which the latitudinal distribution of climate forcings is altered, as is the case for many paleoclimate and other climate experiments.

We give the land masses fictitious names to stress the difference between the model climate and real world climate. This may help keep emphasis on the purposes for which the model is intended, that is, analysis of climate mechanisms, rather than on climate impacts in specific real world regions, which are often subject to misinterpretation.

Our purpose here is to define the Wonderland model and document its performance using climatological sea surface temperatures, illustrating that performance of the atmospheric component is comparable to that of the parent model II. Although the physics of model II is old, documentation of the Wonderland model is needed because it is used for several climate studies [*Hansen et al.*, 1993, 1995, this issue]. Calculation of ocean temperature in the Wonderland model is handled in a simple way, as defined by *Hansen et al.* [this issue].

The Wonderland model is described in section 2. Section 3 is a summary of the climatology of the Wonderland model, based on control run 1 with fixed sea surface temperature. In the companion paper [*Hansen et al.*, this issue] we illustrate the potential of the model via a set of climate sensitivity studies for a wide range of radiative forcings.

2. Model Description

The physical representations in the Wonderland model are the same as those in model II, with the minor exceptions specified below. As described in paper 1, the model solves the simultaneous equations for conservation of mass, energy and momentum, and the equation of state on a grid. The differencing schemes for the dynamics do not require viscosity for numerical stability, and thus they can yield reasonably realistic results with coarse resolution. Radiation is computed with a semi-implicit spectral integration, including all significant atmospheric gases, aerosols, and cloud

Paper number 96JD03435.
0148-0227/97/96JD-03435$09.00

particles. Cloud cover and vertical distribution are computed, but no liquid water budget is kept and the cloud optical properties are fixed. Convection mixes moisture, heat, and momentum, with buoyant air allowed to rise to a height determined by its buoyancy, but the nature of the convection is simple, for example, not including entrainment of environmental air. Surface fluxes are approximated based on a simple drag law formulation and parameterization of the Monin-Obukhov similarity relations. Ground temperature calculations include diurnal variation and seasonal heat storage. Ground hydrology incorporates a water-holding capacity based on local vegetation, but many aspects of the hydrology are arbitrary and are not expected to accurately simulate biospheric effects.

The geography of Wonderland is shown in Figure 1. Most continents resemble a terrestrial counterpart, but their area is constrained so that the zonal mean land cover is the same as on Earth. Surface properties and topography of Wonderland grid boxes are specified to be the same as certain grid boxes in model II, as shown in Figure 2. The sea surface temperatures for control run 1 were adjusted slightly at each latitude as necessary to yield the same zonal mean sea surface temperature as in model II. Note that although the properties of Tropicana are based on Africa, the Wonderland continent has only about half the east-west dimension of the terrestrial continent. Northland, on the other hand, has about the same dimensions as North America.

The model structure at a grid box is the same as in model II, as illustrated schematically in Figure 3. Each grid box has a fraction of land and ocean, as specified in Figure 4a. The mean topography for each grid box (Figure 4b) is the same as for its model II counterpart, and thus the zonal mean topography is not identical to model II, as shown by comparison with Figure 13 of paper 1.

Several specific aspects of the model physics in the Wonderland model differ from those of model II. First, the treatment of water vapor in the fundamental equations is altered so that the effect of water vapor on surface pressure is included in an approximate way, as described in the appendix. The intention of this change is to improve the realism of the surface pressure simulated over an increased range of climate states. Second, radiation calculations are performed at every grid box, rather than at alternate grid boxes as in model II. This change was made to avoid complications in interpretation of radiative forcing experiments with the model. Third, although a 24-hour diurnal cycle is retained, the sector geometry requires an approximation of the solar insolation. This is obtained by letting the Sun rise and set simultaneously at all longitudes, i.e., the time of day is the same throughout Wonderland. Fourth, the calculation of sea ice thickness was altered as described in the appendix. The purpose of this change was to eliminate unrealistic growth of sea ice thickness which occurred at a few grid points in the first trial run with the Wonderland model. Other

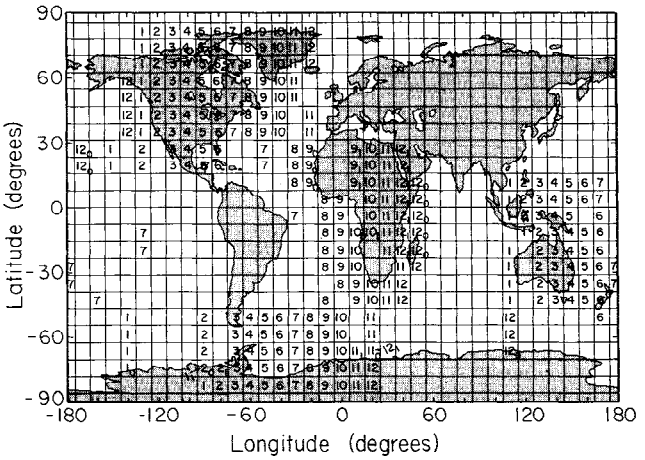

Figure 2. Grid boxes of model II (paper 1) used to specify certain parameters in the Wonderland model. The 12 grid boxes at each latitude of the Wonderland model are numbered west to east, starting with the grid box centered on 60°W (Fig. 1). Subscripts (l and o) are used if the land and ocean fractions of a Wonderland grid box are obtained from two grid boxes of model II.

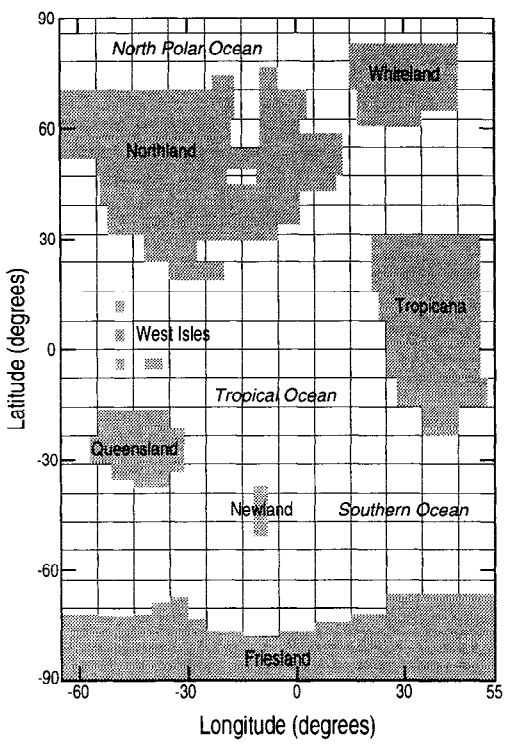

Figure 1. Geography of Wonderland. Grid box edges (7.83° x 10°) are shown over the ocean.

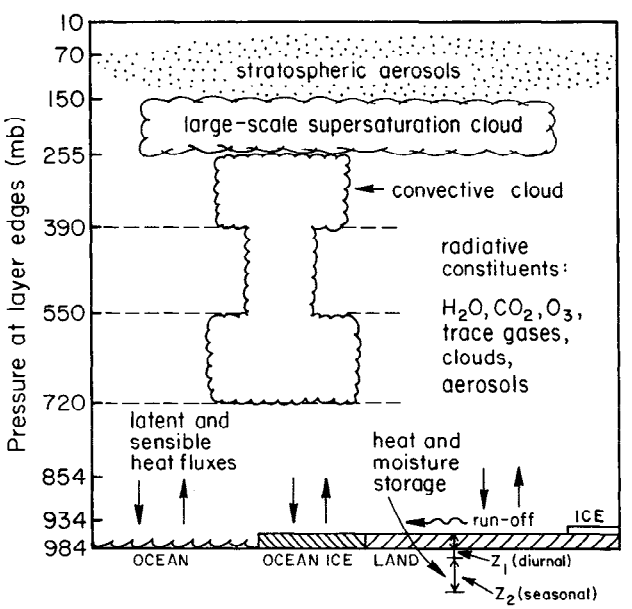

Figure 3. Cartoon of model structure at a grid box. Scale on left gives the global mean pressure at the edges of the nine layers.

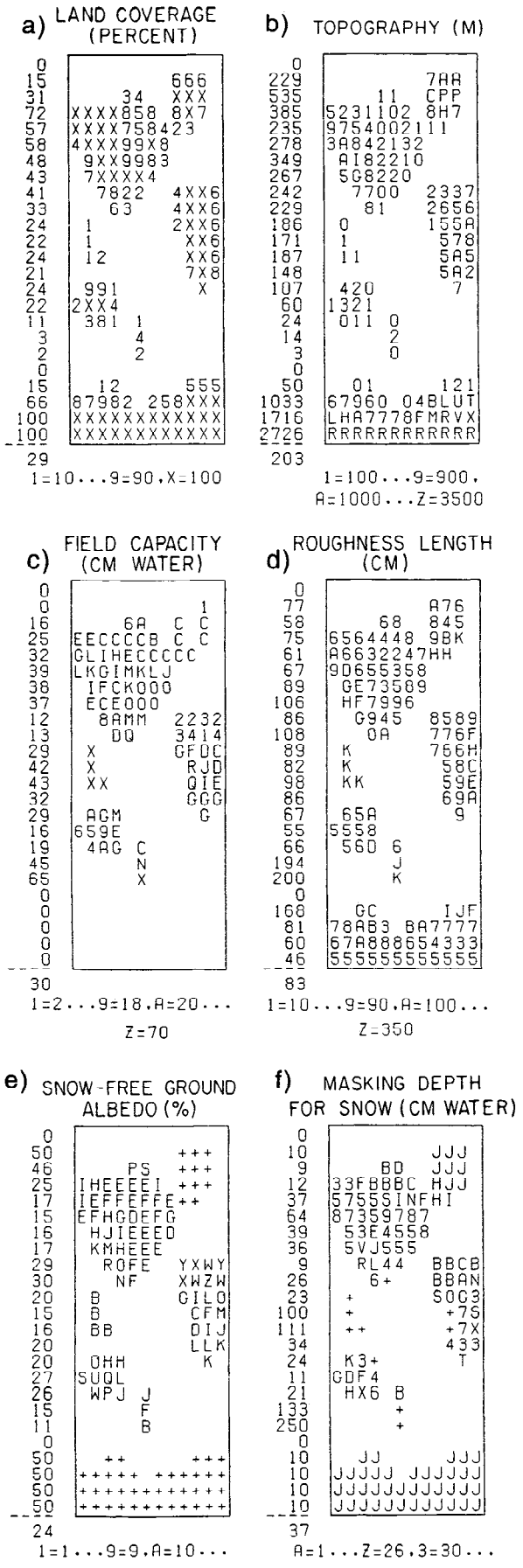

Figure 4. Digital maps of (a) land coverage, (b) topography, (c) total field capacity, (d) roughness length, (e) snow-free ground albedo, and (f) masking depth for snow in the Wonderland climate model. A blank on any map is identically zero. For land coverage 0 is 0-5%, 1 is 5-15%, A is 95-100%, and X is exactly 100%. For topography, 0 is 0-50 m, 1 is 50-150 m and + is more than 3550 m. Zonal means are on the left, above the area-weighted global mean.

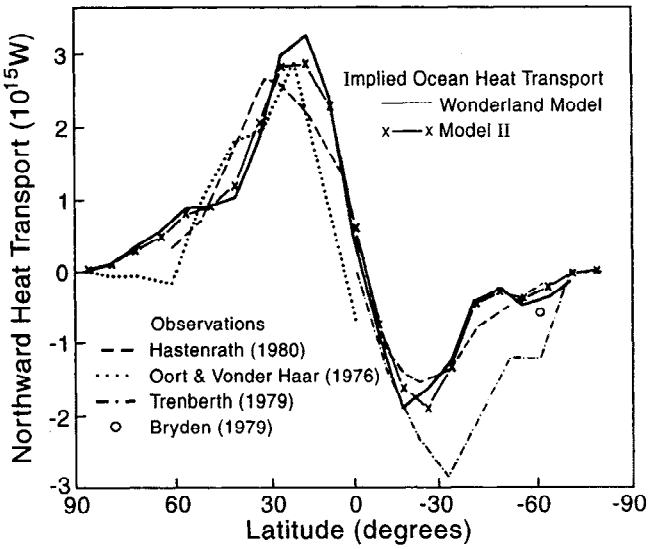

Figure 5. Implied annual ocean heat transport in the Wonderland model (times 3), model II, and observed values.

minor changes were made, as described in the appendix. None of these changes altered the model climatology much, as shown below.

3. Wonderland Climatology

The ocean surface has specified seasonally varying temperature in run 1 based on the climatology of *Robinson and Bauer* [1981] for the grid boxes indicated in Figure 2 but with the ocean temperature adjusted slightly as needed to yield the same zonal mean as for the full 360° of longitude of the real world. Thus the ocean is a potentially unlimited source or sink of heat and water vapor, and the magnitude of these fluxes provides one useful model diagnostic. The implied meridional ocean heat transport, required for the ocean temperature to be the same each year, is shown in Figure 5. The implied transport in the Wonderland model is similar to that in model II and to uncertain observations for the real world.

The zonal mean temperature, zonal wind, and mass stream function are shown in Figure 6 for the December-January-February (DJF) and June-July-August (JJA) seasons. These can be compared to results of model II and observations shown in Figures 20, 29, and 31 of paper 1. The winter low level temperature inversion at high latitudes is too weak in the Wonderland model, and the summer high latitude stratosphere is too cold, the latter problem shared with many other models. The meridional circulation, in both the Hadley and Ferrel cells, is weaker than observed but similar to model II.

The simulated geographical distributions of surface air temperature, cloud cover, precipitation, and sea level pressure are shown in Figure 7. These can be compared with model II results and observations shown in Figures 21, 26, 28, and 34 of paper 1. The results in the Wonderland model generally are very similar to

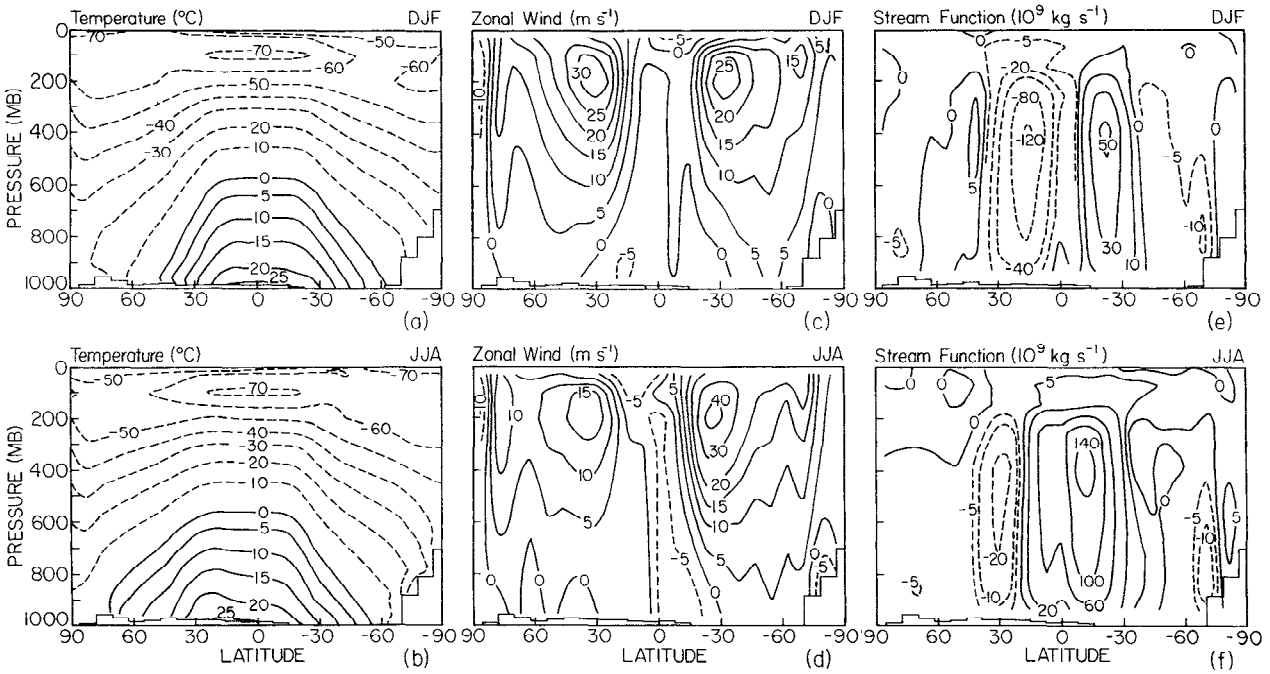

Figure 6. (a) and (b) Zonal mean temperature, (c) and (d) zonal wind, and (e) and (f) mass stream function in the Wonderland model (years 51-100 of run 1). (top) For December-January-February (DJF) and (bottom) for June-July-August (JJA). Compare to observations and model II results in Figures 20, 29, and 31 of paper 1.

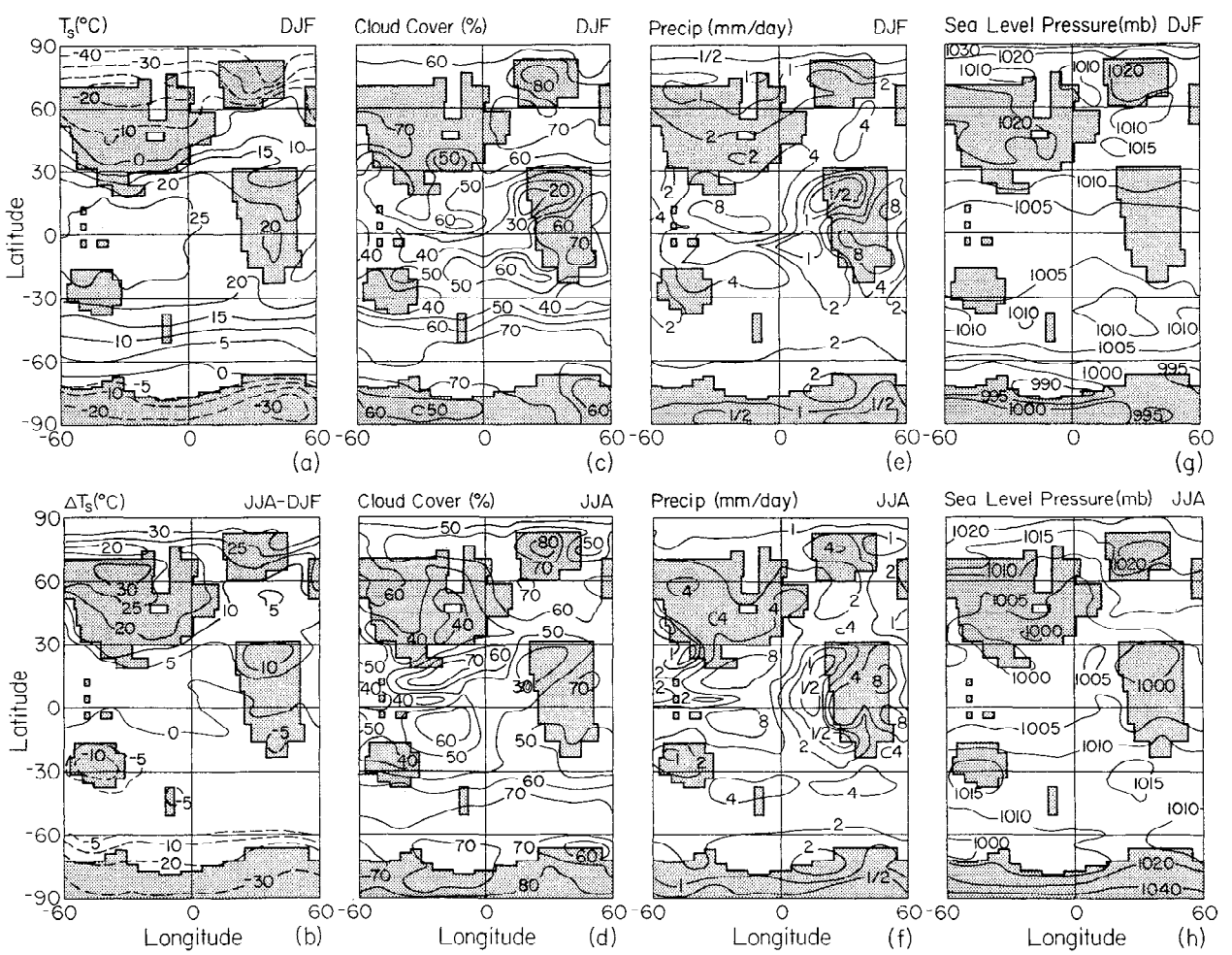

Figure 7. Geographical distributions of (a) and (b) surface air temperature, (c) and (d) cloud cover, (e) and (f) precipitation, and (g) and (h) sea level pressure in the Wonderland model (years 51-100 of run 1). (top) For DJF and (bottom) for JJA, except Figure 7b which shows the difference JJA minus DJF. Compare to Figures 21, 26, 28, and 34 of paper 1. However, note that in regions of high topography we have extrapolated surface pressure to mean sea level pressure (rather than interpolating from nearby regions of low topography, as was done in paper 1 to conform with observational practices), because no observations have been reported from Wonderland.

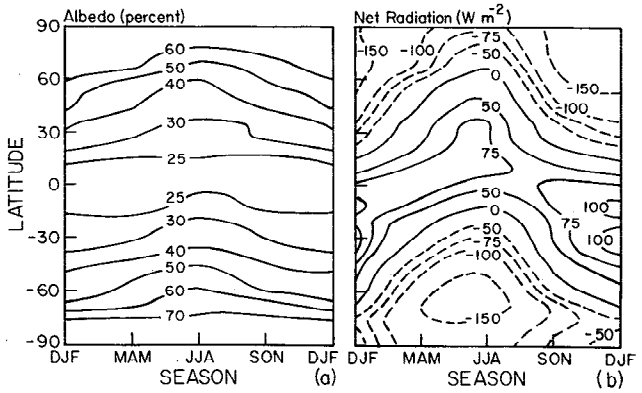

Figure 8. (a) Zonal-mean planetary albedo and (b) net radiation of planet for the Wonderland model (years 51-100 of run 1). Compare to Figure 24 of paper 1.

those in the corresponding grid boxes of model II. In model II the surface air temperature is about 5°C too cool in the midwest United States, apparently a result of unrealistically large moisture holding capacity of the surface and vegetation, a feature which carries over into Northland of the Wonderland model. Excessive precipitation in the central United States and some other regions of model II are also carried over into the Wonderland model. Sea level pressure is several millibars too small in model II at low latitudes and too large at polar latitudes, and the model does not develop sufficiently deep subpolar lows in the southern hemisphere. These characteristics of sea level pressure carry over into the Wonderland model.

The zonal mean planetary albedo and net radiation of the planet are shown in Figure 8 for the Wonderland model. These can be compared with model II results and observations in Figure 24 of paper 1. Model II is in reasonably good agreement with the observations, although the albedo may be a few percent too small at low latitudes. The planetary albedo and net radiation in the Wonderland model are similar to those quantities in model II, but the low-latitude albedo is somewhat larger and thus more realistic.

The surface wind field in the Wonderland model is shown in Figure 9. It features easterly trade winds at low latitudes, westerly flow at middle latitudes and light easterlies at high latitudes, with magnitudes similar to those in model II.

The northward transport of sensible heat, energy and momentum in the Wonderland model is shown in Figure 10 for both the transport by eddies and the total transport. These can be compared with model II results and observations in Figures 37-39 of paper 1. These transports in the Wonderland model are quite similar to the values in model II, but in the northern hemisphere the total energy transports are about 10% larger than in model II as a consequence of the Hadley cell extending further poleward in the Wonderland model (Figure 6).

Finally, in Figure 11 we show the kinetic energy, standing kinetic energy and available potential energy spectra of the northern hemisphere troposphere for model II and the Wonderland model. As expected, since the sector model represents only every third wavenumber on a sphere, there are substantial differences between the Wonderland and model II spectra. The energies tend to be lower in the Wonderland model, particularly for the low wavenumber standing kinetic energy and available potential energy.

4. Discussion

The above results illustrate that the Wonderland model successfully retains most of the climatogical features of the parent climate model II. Of course, it retains the deficiencies of model II, as well, but we anticipate that improvements under development for the global climate model can be incorporated into a new version of the Wonderland model.

The Wonderland model, like its parent climate model II, is designed principally for investigation of the climate response to global radiative forcings. The capabilities for that purpose are illustrated by *Hansen et al.* [this issue] for a wide range of radiative forcings.

Appendix

In this appendix we describe aspects of the model physics which differ between model II (paper 1) and the Wonderland model. As indicated below, there were different reasons for each of these changes.

Water vapor. In the Wonderland model, unlike model II, the amount of water vapor in the air affects the atmospheric density, sensible heat content, and buoyancy, although only in an approximate way. The intention of these changes is to increase the

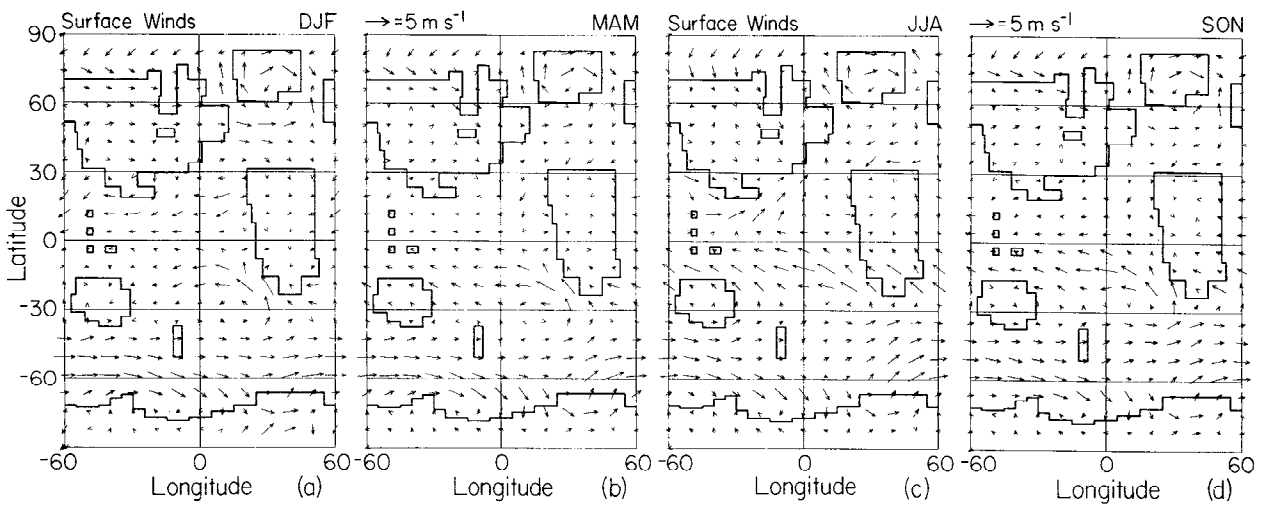

Figure 9. Surface wind speeds in the Wonderland model (years 51-100 of run 1) for (a) DJF, (b) March-April-May (MAM), (c) JJA, and (d) September-October-November (SON). Compare to Figure 30 of paper 1.

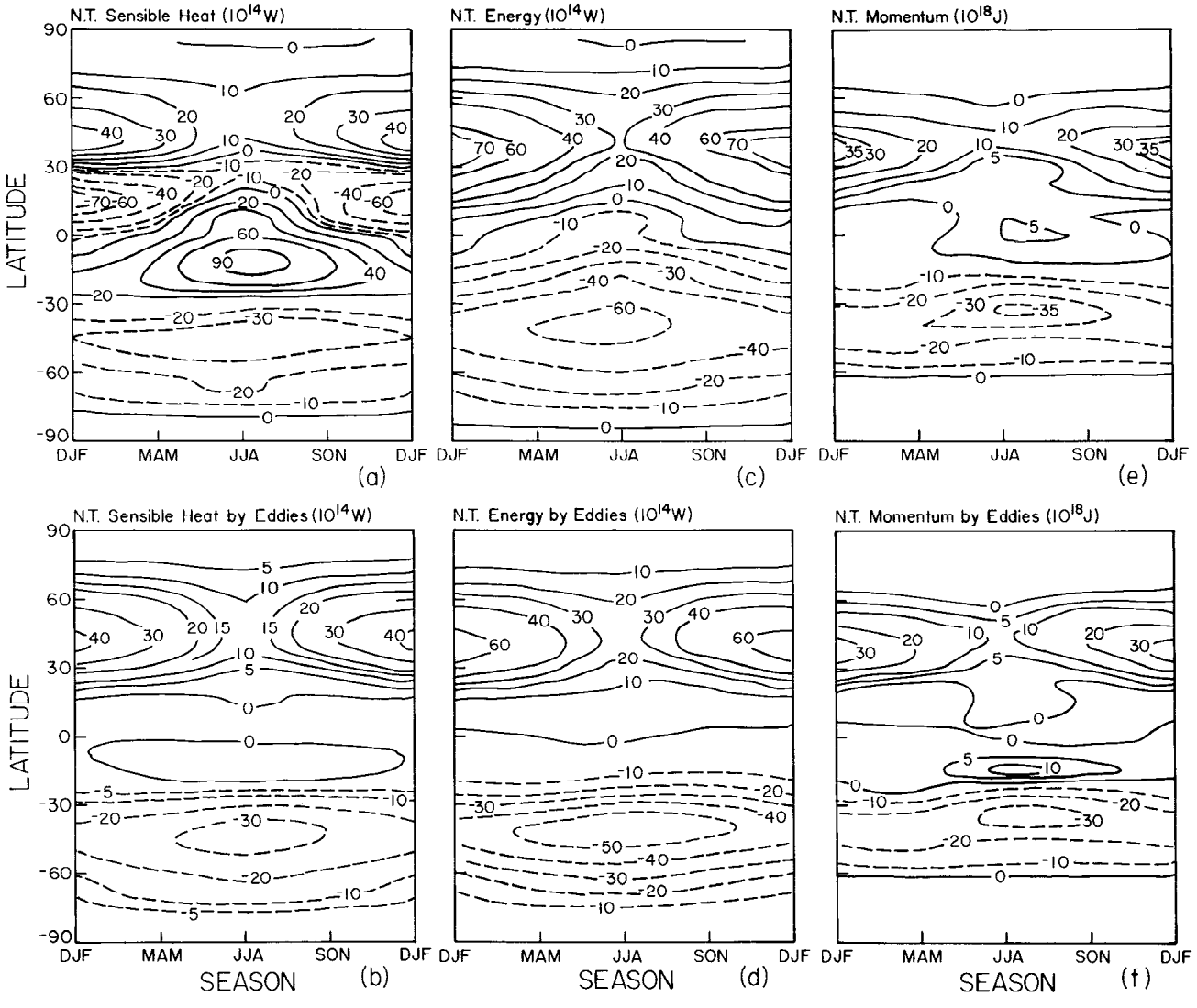

Figure 10. Northward transport of sensible heat, energy and momentum in the Wonderland model (years 51-100 of run 1). The graphs on the top show the total transports and those on the bottom the transports by eddies. Compare to Figures 37-39 of paper 1.

realism of simulations for a climate much warmer than that of today's Earth, specifically for an atmosphere that contains more water vapor. The changes do not have much effect on the model for today's climate.

In model II the atmosphere is treated as a single ideal gas. Thus, with the product of potential temperature and mass conserved under advection, entropy is also conserved. However, this is no longer true for a mixture of two dissimilar ideal gases. Therefore we approximated the properties of water vapor, to make them more similar to dry air. In particular, the specific heat capacity for water vapor was changed from 1911 to 1614 (J/kg °C), so that the ratio of gas constant to specific heat capacity was the same for water vapor and dry air. This change allows both entropy and potential enthalpy to be conserved during advection.

Within this approximation, the water vapor mass is able to affect the pressure gradient force and the atmospheric buoyancy. Moist convection is affected by the buoyancy, and condensation conserves total static energy, including the latent heats of water vapor and ice and the sensible heat of dry air, water vapor, and condensate. Surface interactions also conserve total static energy.

Ocean ice. In the first trial control run of the Wonderland model with computed ocean temperature a trend toward increasing sea ice cover was noted after about 2000 years. This was believed to be a result of some arbitrary specifications regarding sea ice thickness and open water (lead) area in model II. These specifications were modified in the Wonderland model, as described below, to practically eliminate this unrealistic sea ice growth. In future models it would be desirable to incorporate a more physically based representation of sea ice processes.

In model II, if the open ocean tends to cool below -1.6°C, the freezing point, the ocean is kept at -1.6°C and sea ice of 1 m thickness grows horizontally to conserve energy. Horizontal growth of sea ice is limited by a minimum lead fraction in a grid box, which is taken to be $0.1/z$, where z is the ocean ice thickness in meters. After each time step, the open ocean temperature and the ocean temperature beneath the sea ice are mixed to form a single ocean temperature. If the ocean temperature tends to warm above 0°C, it is kept at 0°C and sea ice is melted horizontally. A positive heat flux at the sea ice surface warms the sea ice up to 0°C, with any additional energy melting the sea ice vertically. If the sea ice

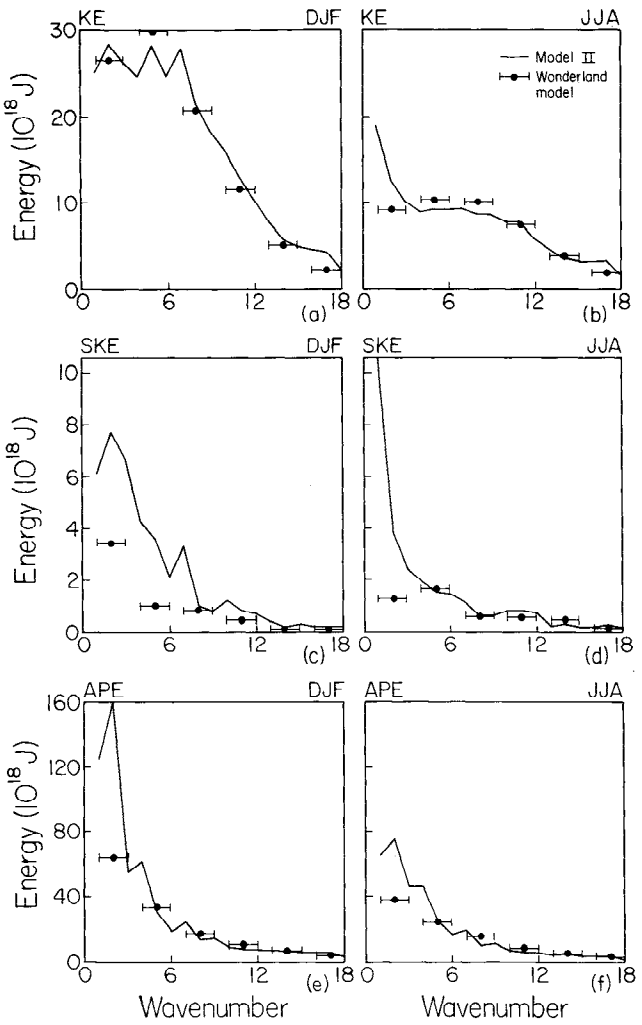

Figure 11. (a) and (b) Kinetic energy, (c) and (d) standing kinetic energy, and (e) and (f) available potential energy spectra of the Northern Hemisphere troposphere in model II (paper 1) and the Wonderland model (years 51-100 of run 1). DJF results are on the left and JJA on the right. Wonderland energies are divided by three, to make the energy per wavenumber interval comparable to model II. Horizontal bars cover the relevant wavenumber range (model II waves 1, 2, 3 for Wonderland wave 1, for example).

tends to become thinner than 1 m, the thickness is held at 1 m with the sea ice melted horizontally.

In the Wonderland model, the initial sea ice thickness is reduced to 0.5 m and the lead area is also reduced. The minimum lead area is 10% for sea ice thickness 0.5 m, and it decreases linearly to zero at a sea ice thickness of 5 m. Also, in the Wonderland model the ocean does not melt sea ice until the temperature warms above 2°C. The ice first melts vertically, until a thickness of 0.5 m is reached, after which it melts horizontally.

Clouds. Clouds are treated in an unrealistically simple fashion in model II and in the Wonderland model. Although large-scale cloud cover is predicted, on the basis of saturated humidity, the cloud optical properties are simply specified (fixed) as a function of layer. The clouds in model II provide a positive climate feedback mechanism, increasing the model sensitivity for doubled carbon dioxide from about 2.7°C to 4.2°C [*Hansen et al.*, 1984]. The cloud feedback in the real world is extremely uncertain. For example, *Mitchell et al.* [1989] have shown that by changing parameters in their cloud formulation they alter the sensitivity of their model from 1.9 to 5.5°C for doubled carbon dioxide.

We allow the cloud feedback in the Wonderland model to be variable, so that the sensitivity of the model to a radiative forcing can be varied in a simple manner. This permits the model to be used for empirical studies of climate sensitivity, by means of comparisons with observed climate changes on different time scales [*Hansen et al.*, 1993]. In the Wonderland model we achieve arbitrary climate sensitivity by multiplying the cloud cover by the factor $(1 + c\Delta T)$, where ΔT is the deviation of global mean temperature from that in an initial control run and c is an empirical constant. For example, we used c = 0.2 and 0.05 to reduce the model sensitivity for doubled carbon dioxide to 0.5 and 1.5°C, respectively. In most experiments with the Wonderland model [*Hansen et al.*, 1995, this issue] we use a small value of c (0.012) to yield a climate sensitivity (3.6°C for doubled CO_2) which is well within the range, 3 ± 1°C, which we infer from empirical evidence [Hansen *et al.*, 1993].

Miscellaneous. In model II, computing time is saved by calculating the radiation only at every second gridbox, with results at other grid boxes specified as the average for neighboring grid boxes. This procedure is a nuisance in analysis of the energetics of a region. Thus in the Wonderland model we calculate the radiation at every gridbox.

Most calculations with model II were carried out on a mainframe computer in "single precision", i.e., with an accuracy of about seven decimals and truncation of remaining digits. Because of the large number of calculations, a noticeable loss of energy could occur [*Hansen et al.*, 1983, 1984]. The Wonderland calculations are carried out on a workstation (IBM RS/6000 series) which has double precision and negligible loss of accuracy.

In model II, kinetic energy lost by moist convection, dry convection, and surface friction disappeared from the model, although it was noted as a diagnostic. In the Wonderland model, this energy is added back as sensible heat after each process.

In the version of model II with calculated ocean temperature a "correction" of solar energy absorbed by the ocean surface is applied to account for the planetary radiation imbalance at the top of the atmosphere in the control run with observed ocean surface temperatures. In the Wonderland model we do not apply any such correction.

Acknowledgments. This work was supported by the NASA Climate and EOS programs. We thank Lilly DelValle and Jose Mendoza for drafting the figures, and Christina Koizumi and Ely Duenas for desktop publishing.

References

Bryden, H. L., Poleward heat flux and conversion of available potential energy in the Drake Passage, *J. Mar. Res.*, 37, 1-22, 1979.

Hansen, J., G. Russell, D. Rind, P. Stone, A. Lacis, S. Lebedeff, R. Ruedy and L. Travis, Efficient three-dimensional global climate models for climate studies: models I and II, *Mon. Wea. Rev., 111*, 609-662, (paper 1), 1983 .

Hansen, J., A. Lacis, D. Rind, G. Russell, P. Stone, I. Fung, R. Ruedy, and J. Lerner, Climate sensitivity: analysis of feedback mechanisms, in *Climate Processes and Climate Sensitivity, Geophys. Monogr. Ser.*, vol. 29, pp. 130-163, edited by J. E. Hansen and T. Takahashi, AGU, Washington, D.C., 1984.

Hansen, J., A. Lacis, R. Ruedy, M. Sato, and H. Wilson, How sensitive is the world's climate?, *Natl. Geogr. Res. Explor., 9*, 142-158, 1993.

Hansen, J., M. Sato, and R. Ruedy, Long-term changes of the diurnal temperature cycle: Implications about mechanisms of global climate change, *Atmos. Res., 37*, 175-209, 1995.

Hansen, J., M. Sato, and R. Ruedy, Radiative forcing and climate response, *J. Geophys. Res.*, this issue.

Hastenrath, S., Heat budget of tropical ocean and atmosphere, *J. Phys. Oceanogr.*, 10, 159-170, 1980.

Lorenz, E.N., Deterministic nonperiodic flow, *J. Atmos. Sci., 20,* 130-141, 1963.

Manabe, S., Climate and ocean circulation, 1, The atmospheric circulation and the hydrology of the Earth's surface, *Mon. Weather Rev., 97,* 739-774, 1969.

Mitchell, J. F. B., C.A. Senior, and W.J. Ingram, CO_2 and climate: A missing feedback?, *Nature, 341,* 132-134, 1989.

Oort, A. H., and T. H. Vonder Haar, On the observed annual cycle in the ocean-atmosphere heat balance over the Northern Hemisphere, *J. Phys. Oceanogr., 6,* 781-800, 1976.

Robinson, M., and R. Bauer, Oceanographic monthly summary, 1, no. 2, pp. 2-3, NOAA Natl. Weather Serv., Washington, D.C., 1981.

Trenberth, K. E., Mean annual poleward energy transports by the oceans in the Southern Hemisphere, *Dyn. Atmos. Oceans,* 4, 57-64, 1979.

J. Hansen, A. Lacis, J. Lerner, D. Rind, R. Ruedy, G. Russell, and M. Sato, NASA Goddard Institute for Space Studies, 2880 Broadway, New York, NY 10025. (e-mail: jhansen@giss.nasa.gov; alacis@giss.nasa.gov; jlerner@giss.nasa.gov; drind@giss.nasa.gov; rruedy@giss.nasa.gov; grussell@giss.nasa.gov; makis@giss.nasa.gov;)

P. Stone, Center for Meteorology and Physical Occanography, Massachusetts Institute of Technology, Cambridge, MA 02139. (e-mail: phstone@mit.edu)

(Received July 8, 1996; revised October 29, 1996;
accepted October 29, 1996.)